Fall 2018

Inferring species origin through virtual histology: A comparison of third metapodials from Homo sapiens and Ursus americanus using Micro-computed Tomography

Hannah Stephen
hes47@zips.uakron.edu

IInferring species origin through virtual histology: A comparison of third metapodials from *Homo sapiens* and *Ursus americanus* using Micro-computed Tomography

Honors Thesis

Presented to

The Honors College at The University of Akron

In Partial Fulfillment

of the Requirements for the Degree

Bachelor of Science (Honors)

HANNAH STEPHEN

December, 2018

TABLE OF CONTENTS

I.Introduction

Bone identification is a vital aspect in the field of forensic anthropology. The misidentification of species based on their bone morphology can result in detrimental mistakes that lead to the misidentification of humans with nonhuman mammals (Mulhern 2016). Similar to many other mammals, the black bear (*Ursus americanus*) front paws and the human hands are made up of phalanges, metacarpals, and carpal bones and the black bear hind paws and the human feet are made up of the phalanges, metatarsal, and tarsal bones. Without their claws, black bear paw metapodials are remarkably similar to human hands/feet on the gross anatomical scale. When black bear skeletal remains are discovered they can be misidentified as being human, especially when only fragments of the bone are recovered (Harrison 2012). There is well-documented macroscopic evidence to support the morphological similarities of black bear and human metacarpals and metatarsals, but for identification purposes past research is only useful when the entirety of a bone is recovered. The current literature focuses on the gross macrostructural characteristics across the whole metatarsal or metacarpal (Dominguez and Crowder 2012). When a partial section is recovered, however, identification can be a challenge because there are many similarities in the macrostructure of distinct mammals. Many professionals (e.g., law enforcement) are not experts in the recognition of mammalian metapodial identification (Smart 2009). As such, when skeletal remains are highly fragmented/and or commingled, standard macroscopic approaches can prove insufficient. In these scenarios, bone fragment identification methods shift from a gross level to the microstructural to provide a more definitive analysis. Up to this point, there is a lack of literature that compares the histological similarities of human and black bear metacarpals and metatarsals on a quantitative microstructural level (Mulhern 2016). This causes difficulty in an identification of species origin beyond the gross anatomy and can cause uncertainty in forensic identification.

The similar morphology between the two species served as the foundation to investigate: (1) the microstructural differences between human and black bear metacarpals and metatarsals using a non-destructive three-dimensional (3D) approach, and (2) microstructural data that will aid in species identification efforts when bone fragments are discovered in a forensic context.

This study specifically analyzed metacarpal and metatarsal cortical bone porosity by measuring quantitative parameters: total (“volume of interest (VOI)”), volume (TV), total canal volume within VOI (Ca.V), canal number (Ca.N), average canal diameter (Ca.Dm), and cortical porosity (Ca.V/TV) to identify if microstructural similarities exist that match the gross anatomy between black bears and humans. There was also an analysis of qualitative parameters: bone composition (e.g., woven, fibrolamellar, Haversian), osteon banding, and resorptive spaces. The quantitative measurements were conducted using micro-Computed Tomography imaging (micro-CT) on the third metacarpals and metatarsals of both the human hands/feet and the black bear front/hind paws. This modern advanced imaging technology provided many benefits that were unable to be performed in the past. Micro-CT allows for a non-invasive and non-destructive scan to produce a 3D reconstruction of the cortical porosity of the bone. This is important because this technique is non-destructive, allowing for the scanned specimens to remain unaltered and used in the future. The results of the measured parameters provided quantitative data that compared the microstructural similarities that, when paired with the well-documented macrostructural similarities between the two species, can limit the discrepancies made in forensic identification.

II. Materials/Methods

The third metacarpals and metatarsals from the black bear paws and the human hands/feet were used to create 3D renders using micro-CT. The bear metapodials, a sample size of 6 ($n = 6$), (**Figure 1**) were loaned from the Vertebrate Zoology Department at the Cleveland Museum of Natural History. The human metapodials, a sample size of 10 ($n = 10$), were obtained from cadaveric specimens from the University of Toledo, College of Medicine and Life Sciences and The University of Akron's skeletal teaching collection, housed in the Department of Biology. The human cadaveric specimens (**Figure 2**) were cleaned using a water and Tergazyme solution to remove soft tissues that would cause unwanted artifacts in the 3D scans. All samples were fixed in a 70% ethanol solution and subsequently dried.

Micro-CT scanning was carried out at The University of Akron's Polymer Innovation Center via a SkyScan 1172 (Bruker, Kontich, Belgium) desktop X-ray system (**Figure 3**). Each bone was mounted on a brass peg and inserted into the X-ray system (**Figure 4**). Before the scans were obtained, flat and dark field projections were obtained to prevent unwanted noise in the detector and X-ray beam. The SkyScan 1172 (Bruker, Kontich, Belgium) system imaged the metapodials by rotating around the object at 180 degrees of rotation until a collection of projections spanning the midshaft of the bone were produced (**Figures 5 and 6**). A set of parameters were established and applied to each scan: X-ray settings of 100 kV and 100 μA, a source spot size of 5.5 μm, an 8.83 camera pixel size, a rotation step of 0.20 degrees, 5-frame averaging, and a combined aluminum and copper filter. The projections were then reconstructed using NRecon 1.6.10.2 (Bruker, Kontich, Belgium), a projection-based reconstruction software package. NRecon cleared the images of any ring and beam hardening artifacts (**Figures 7 and 8**). From the whole image stack, a smaller, circular Volume of Interest (VOI) was taken from an anterior section of each bone. The

VOI image stacks were analyzed using CTAnalyser 1.15.4.0 (Bruker, Kontich, Belgium), following a protocol described by Andronowski and colleagues (2017). The variables that were measured by CTAnalyser include: total (“volume of interest (VOI)”) volume (TV), total canal volume within VOI (Ca.V), canal number (Ca.N), average canal diameter (Ca.Dm), and cortical porosity (Ca.V/TV). The final step taken to obtain the quantitative data was to conduct statistical analyses using SPSS 23.0 statistical software (Chicago, IL, USA). Statistical analyses were conducted to test whether species origin had a significant effect on the quantitative parameters using independent *t*-tests with a significance of $p \leq 0.05$. A squared regression (r) value was further calculated for each analyzed metapodial to test for the fraction of variance between the compared parameters. Qualitative data were obtained by visual comparisons among the image stacks. The qualitative variables analyzed included: bone composition (e.g., woven, fibrolamellar, Haversian), osteon banding, and resorptive spaces. All data were compiled in tables for comparison.

III. Results

To test whether the species and genetic makeup has an effect on the total (“volume of interest (VOI)”) volume (TV), total canal volume within VOI (Ca.V), canal number (Ca.N), average canal diameter (Ca.Dm), and cortical porosity (Ca.V/TV) independent *t*-tests (comparisons between species) were performed at a significance of $p \leq 0.05$. Descriptive statistics were obtained, and a normality test resulted in a rejection of the normality of the data. To correct this issue, a log transformation was performed on the variables. Nonparametric tests were conducted at a significance of $p \leq 0.05$. The independent *t*-tests demonstrated that the canal number (Ca.N) was significantly different between black bear and human metacarpals and metatarsals (t = 3.971; p= <0.05) (**Table 1**). The independent *t*-tests also demonstrated that the canal number (Ca.N) was significantly different when metacarpals were compared between species (t = 3.178; p= <0.05) (**Table 2**). The quantitative comparison of the metatarsals between the species did not show a significant difference (**Table 3**). For the average canal diameter (Ca.Dm), the total (“volume of interest (VOI)”) volume (TV), total canal volume within VOI (Ca.V), and the cortical porosity (Ca.V/TV), there was not a significant contrast between the bear and human metapodials. The paired *t*-tests also produced a linear regression for each variable. The squared regression value did not show a significance for the measured variables. For the qualitative analysis, the resorptive spaces and osteon banding were more prevalent in the bear metacarpals and metatarsals (**Table 4**). Qualitative results revealed that the human metacarpals and the metatarsals exhibited Haversian bone composition. The bear metapodials displayed both plexiform and Haversian bone composition (**Tables 5 and 6**). In the bear metapodials, the majority of osteon banding was present within the periosteal bone envelope. Plexiform bone follows a brick-like pattern and can be seen as distinct brick-like layers along the periphery. **Figure 7** demonstrates osteon banding on the periosteal region and plexiform bone composition that follows the layered banding pattern.

IV. Discussion

The bone microstructural data presented here can act as a vital source in the field of forensic anthropology. To our knowledge, this work represents the first examination of 3D microstructural variation in human versus black bear metapodials. Past documentation focused on the gross anatomical similarities between black bears and humans (Dominguez and Crowder 2012). The data was useful in demonstrating the gross resemblances that black bears and humans exhibit in their metapodial structures. The lack of microstructural studies, however, represent a significant literature gap. The previous literature (Hillier and Bell 2007) compares the histological analysis of compact bone of various species such as cat, dog, cow, horse, and bear.

Research measured the microstructural data of species of a range of sizes including larger species such as a bear and smaller species such as a cat. This lead to the qualitative analysis of the bone of larger mammals exhibiting both Haversian and plexiform bone tissue, and smaller mammals exhibiting Haversian bone tissue alone. These findings support our qualitative bone composition data where the black bears exhibit both plexiform and Haversian bone tissue and the humans only exhibit Haversian tissue. Further studies (Mulhern and Ubelaker 2001) have quantitatively compared the Haversian systems of smaller nonhuman mammals from humans with a focus on osteon banding.

Owing to our collected data, fragmented metapodial identification will now have a reliable and accurate source of collected data for species comparisons if they are suspected to be human. Comparable to the macrostructural data, there were many similarities between the microstructural data of black bears and humans. The total volume, total canal volume within VOI, average canal diameter, and cortical porosity were closely related between the species. These variables did not show a significant difference. The measurement of canal number between the species did show significance. The variation in the canal number demonstrated that there was a much greater number of canals in the black bears than there were in the human bone microarchitecture. The difference in canal number can be used in future forensic anthropological analyses to accurately identify a black bear metapodial fragment from human fragment using either traditional histological methods or micro-CT. Limitations of this study include a small sample size, due to the museum specimen availability. Thus, in the future further data should be collected comparing a larger sample of black bear and human metapodials to strengthen the findings. These data will bring new sources for confident identification of metapodials especially when fragmented bone is encountered. There should also be a microstructural data set compiled which compares humans and other mammalian species that display similarities in their gross anatomical structures. Further describing nonhuman mammalian bone microarchitecture will narrow the gap for species clarification and reduce the challenges for anthropologists when mammalian bone fragments are recovered in a forensic context.

V. Conclusions

This study focused on the hypothesized microstructural similarities (e.g., cortical porosity, average canal diameter, and canal number total) that are exhibited between black bear and human metapodials. The two mammals are similar on the gross anatomical scale, and so these data aimed at benefiting the forensic science community through simpler species identification. The 3D renders of the third metapodials were produced through a non-destructive method that allowed for detailed analysis, and both qualitative and quantitative comparisons. Results demonstrated differences between the human and black bear metacarpals and metatarsals, supporting the hypothesis that a microstructural comparison is necessary for moving forward towards the fragmentary bone identification of human and bear metapodials. From this point forward, there will be greater confidence in identifying nonhuman mammal versus human bone tissue as the microstructural parameters are distinguishable.

References

Andronowski JM, Mundorff AZ, Pratt IV, Davoren JM, Cooper DML. 2017. Evaluating differential nuclear DNA yield rates and osteocyte numbers among human bone tissue types: A synchrotron micro-CT approach. Forensic Science International: Genetics (28): 211-218.

Dominguez VM, Crowder CM. 2012. The utility of osteon shape and circularity for differentiating human and nonhuman Haversian bone. American Journal of Physical Anthropology. 147 (Supplement 54): 133.

Harrison KD. 2012. Inferring mode of locomotion through microscopic cortical bone analysis: A comparison of the third digits of homo sapiens and ursus americanus using micro-CT [Master's thesis]. University of Manitoba. Department of Anthropology. 110 p.

Hillier ML, Bell LS. 2007. Differentiating human bone from animal bone: A review of histological methods. Journal of Forensic Sciences. 52: 249-63.

Mulhern DM. 2016. Differentiating human from nonhuman skeletal remains. In: Crowder C, Stout S, editors. Handbook of forensic anthropology and archaeology. Boca Raton: CRC Press. p. 109-134

Mulhern DM, Ubelaker DH. 2001. Differences in osteon banding between human and nonhuman bone. Journal of Forensic Sciences. 46: 220-2.

Smart TS. 2009. Carpals and tarsals of mule deer, black bear and human: An osteology guide for the archaeologist [dissertation]. Western Washington University. 114 p.

Appendix A: Figures

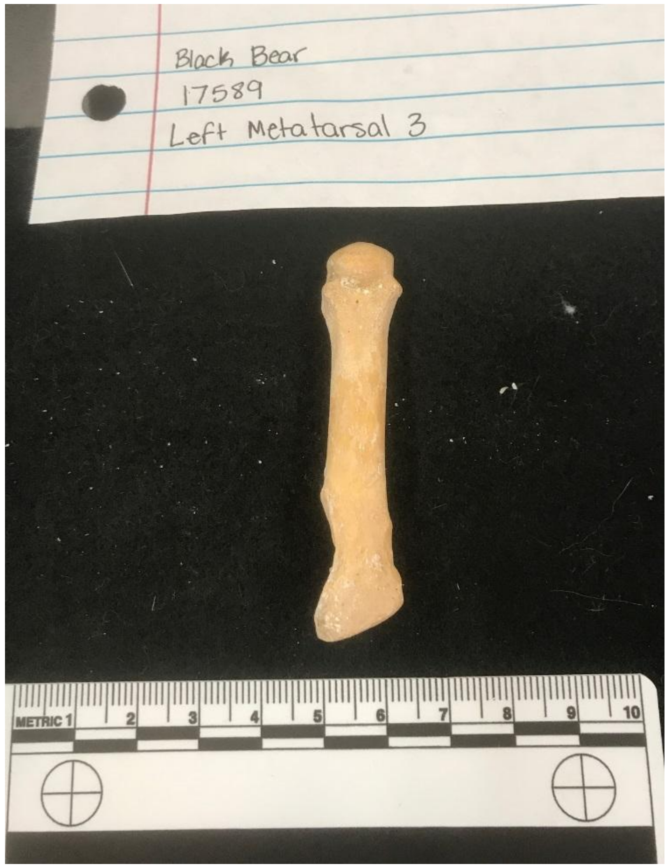

Figure 1: Black bear left third metatarsal

Figure 2: Human third metatarsal.

Figure 3: SkyScan 1172 micro-CT laboratory X-ray system housed at The University of Akron's Polymer Innovation Center

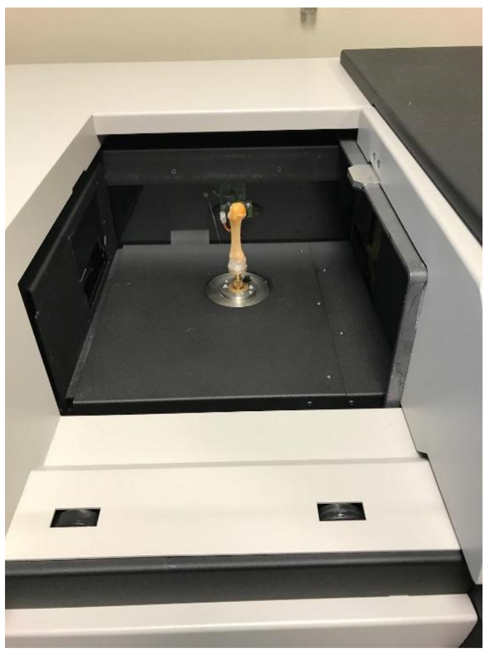

Figure 4: Human left third metatarsal inside the SkyScan micro-CT X-ray system

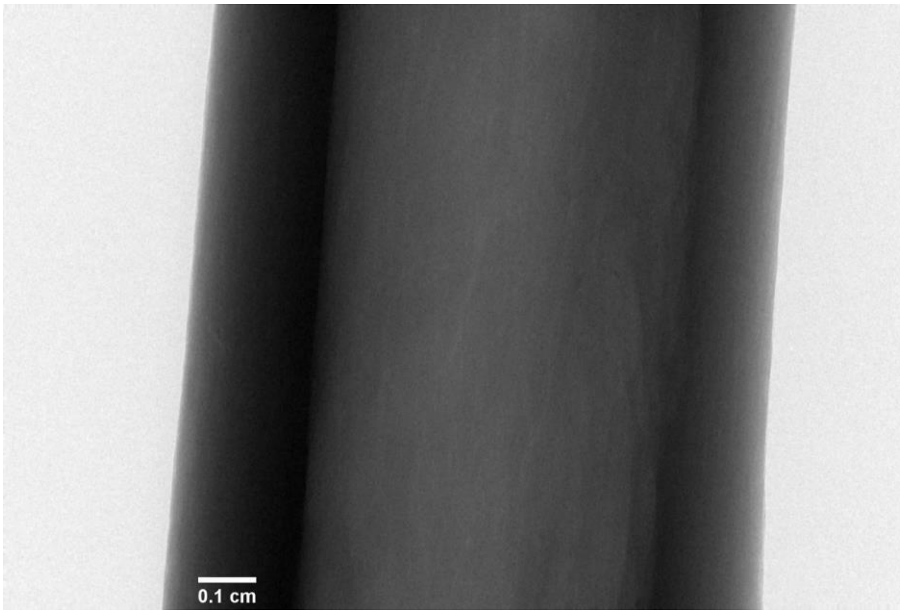

Figure 5: Black bear left third metatarsal reconstructed image stack from the micro-CT imaging

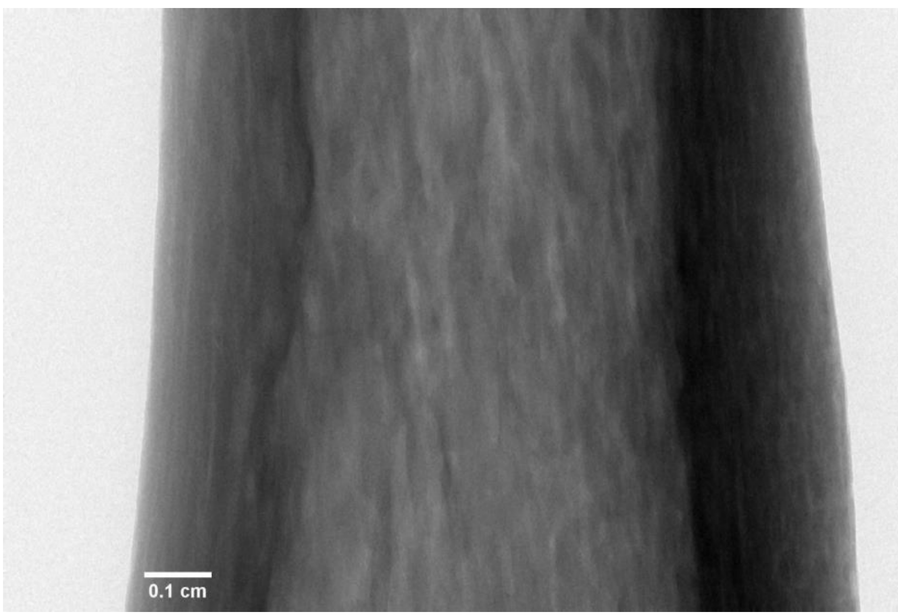

Figure 6: A reconstructed image stack of a human left third metatarsal from the micro-CT imaging

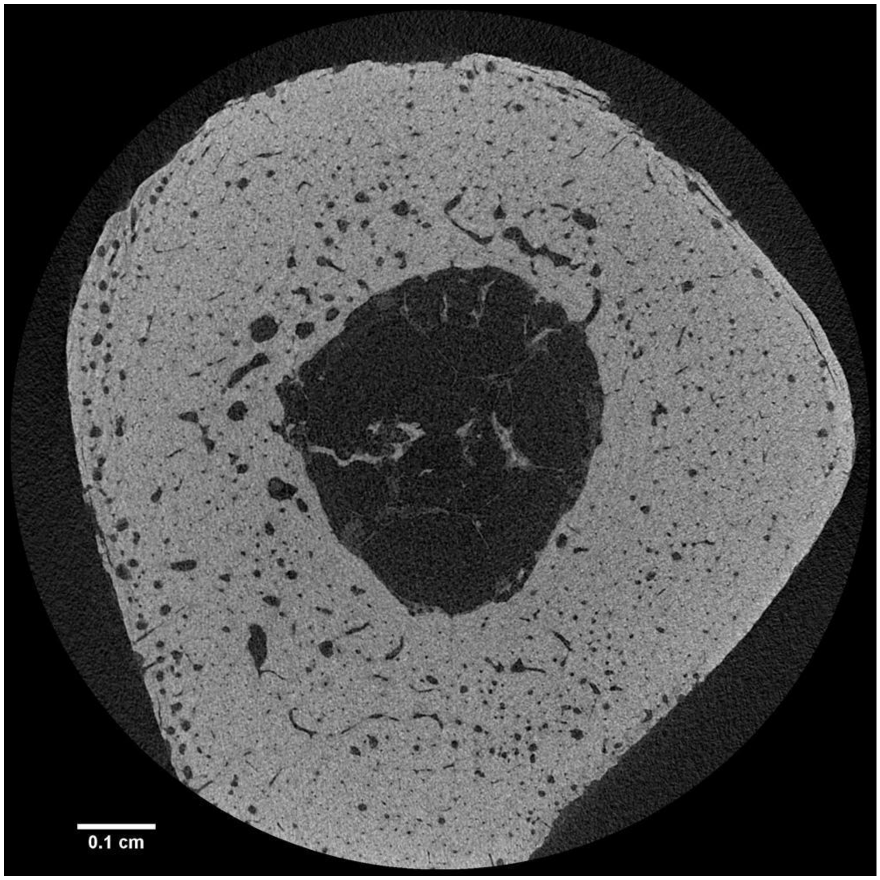

Figure 7: Single slice from a 3D image stack of a black bear left third metatarsal

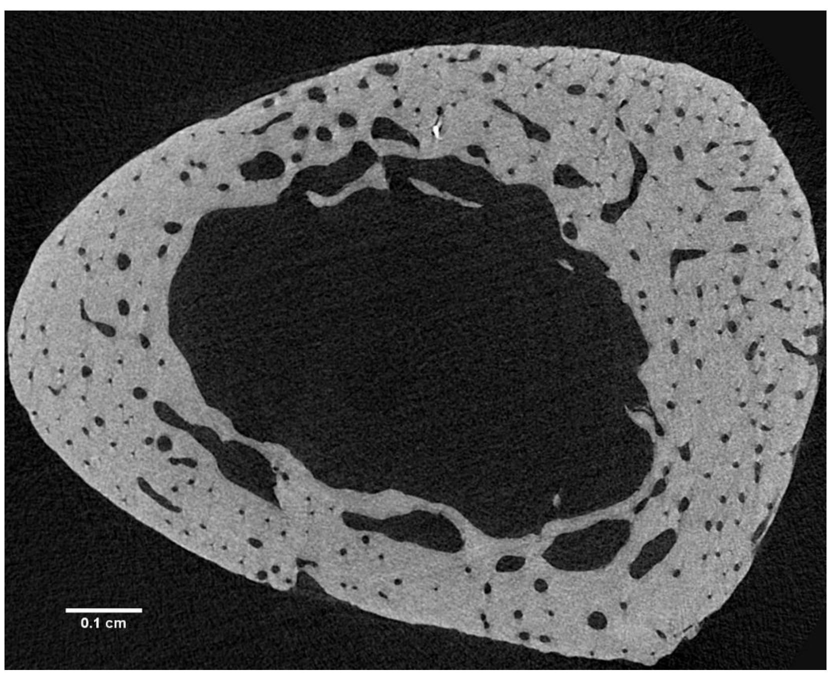

Figure 8: Single slice from a 3D image stack of a human left third metatarsals

Appendix B: Tables

Table 1: Average measurements of both metacarpals and metatarsals categorized by species

Average Quantitative Measurements of Metapodials by Species			
	Unit	Black Bear	Human
Total VOI volume (TV)	μm^3	$4.21 \times 10^9 \pm 0.00$	$3.98 \times 10^9 \pm 4.76 \times 10^8$
Total Canal Volume within VOI (Ca. V)	μm^3	$1.49 \times 10^9 \pm 7.48 \times 10^8$	$1.20 \times 10^9 \pm 5.90 \times 10^8$
*Canal number (Ca. N)	μm^3	974 ± 678	243 ± 397
Average Canal Diameter (ca. Dm)	µm	$1.36 \times 10^2 \pm 68.0$	$1.21 \times 10^2 \pm 49.3$
Cortical Porosity (Ca.V/TV)	%	35.4 ± 17.8	28.7 ± 13.5

Table 2: Measured parameters of metacarpals categorized by species

Average Quantitative Measurements of Metacarpals by Species			
	Unit	Black Bear	Human
Total VOI volume (TV)	μm^3	$4.21 \times 10^9 \pm 0$	$3.98 \times 10^9 \pm 5.04 \times 10^8$
Total Canal Volume within VOI (Ca. V)	μm^3	$1.19 \times 10^9 \pm 1.10 \times 10^1$	$1.27 \times 10^9 \pm 6.90 \times 10^8$
*Canal number (Ca. N)	μm^3	$920 \pm 1.01 \times 10^3$	90.4 ± 107
Average Canal Diameter (ca. Dm)	µm	$1.08 \times 10^2 \pm 2.47$	$1.32 \times 10^2 \pm 67.4$
Cortical Porosity (Ca.V/TV)	%	28.3 ± 1.26	30.4 ± 16.0

Table 3: Measured parameters of metatarsals categorized by species

Average Quantitative Measurements of Metatarsals by Species			
	Unit	Black Bear	Human
Total VOI volume (TV)	μm^3	$4.21 \times 10^9 \pm 0$	$3.98 \times 10^9 \pm 5.04 \times 10^8$
Total Canal Volume within VOI (Ca. V)	μm^3	$1.19 \times 10^9 \pm 1.06 \times 10^9$	$1.27 \times 10^9 \pm 5.40 \times 10^8$
Canal number (Ca. N)	μm^3	1028 ± 337	395.4 ± 534
Average Canal Diameter (ca. Dm)	µm	$1.64 \times 10^2 \pm 95.0$	$1.09 \times 10^2 \pm 21.7$
Cortical Porosity (Ca.V/TV)	%	42.6 ± 25.2	27.1 ± 12.1

Table 4: Measured qualitative parameters of metapodials categorized by species

Average Qualitative Measurements of Metapodials by Species		
	Black Bear	**Human**
Bone Composition	Plexiform and Haversian Bone	Haversian Bone
Osteon Banding	Present	Present
Resorptive Spaces	*Variably Present	Not Present

Table 5: Measured qualitative parameters of metacarpals categorized by species

Average Qualitative Measurements of Metacarpals by Species		
	Black Bear	**Human**
Bone Composition	Plexiform and Haversian Bone	Haversian Bone
Osteon Banding	Present	Present
Resorptive Spaces	Not Present	Present

Table 6: Measured qualitative parameters of metatarsals categorized by species

Average Qualitative Measurements of Metatarsals by Species		
	Black Bear	**Human**
Bone Composition	Plexiform and Haversian Bone	Haversian Bone
Osteon Banding	Present	Present
Resorptive Spaces	Present	Not Present